Microstructures and Mechanical Properties of Transient Liquid-Phase Diffusion-Bonded Ti$_3$Al/TiAl Joints with TiZrCuNi Interlayer

H.S. REN, H.P. XIONG, S.J. PANG, B. CHEN, X. WU, Y.Y. CHENG, and B.Q. CHEN

Transient liquid-phase diffusion bonding of Ti$_3$Al-based alloy to TiAl intermetallics was conducted using Ti-13Zr-21Cu-9Ni (wt pct) interlayer foil. The joint microstructures were examined using a scanning electron microscope (SEM) equipped with an electron probe micro-analyzer (EPMA). The microhardness across the joint was measured and joint strengths were tested. The results show that the Ti$_3$Al/TiAl joint mainly consists of Ti-rich phase, Ti$_2$Al layer, α_2-Ti$_3$Al band, and residual interlayer alloy dissolved with Al. The amount of residual interlayer at the central part of the joint is decreased with the increase of the bonding temperature, and meantime the Ti$_2$Al and α_2-Ti$_3$Al reaction bands close to the joined Ti$_3$Al-based alloy become thickened gradually. Furthermore, the central part of the joint exhibits the maximum microhardness across the whole joint. The joints bonded at 1193 K (920 °C) for 600 seconds with a pressure of 2 MPa presented the maximum shear strength of 417 MPa at room temperature, and the strength of 234 MPa was maintained at 773 K (500 °C).

I. INTRODUCTION

TITANIUM aluminides are one of the most promising intermetallic compounds, and a lot of attempts have been made to develop their applications in the past decades.[1] In particular, Ti$_3$Al-based alloy is a structural material with a potential for applications in aerospace field due to its relatively low density, high specific strength, excellent creep behavior, and good oxidation stability at high temperature.[2,3] To realize its practical application, developing joining technologies of Ti$_3$Al-based alloy to itself or to other materials such as TiAl intermetallics has become an important issue.

Fusion welding, brazing, and diffusion bonding have been used to join Ti$_3$Al-based alloys. For instance, Wu et al. studied the joining of Ti-24Al-17Nb (at. pct) alloy using laser beam welding technology and the joint strength at room temperature was equivalent to that of the base material.[4] The dissimilar joining of Ti-22Al-25Nb (at. pct) to Ti-6.5Al-3.5Mo-1.5Zr-0.3Si (wt pct) alloys was conducted using electron beam welding technique in Reference 5, and the joint strength

was even higher than that of base material. Moreover, Cadden et al.[6] investigated the brazing of Ti-13.4Al-21.2Nb (at. pct) alloy using Ti-Cu-Ni system fillers. Commercial laminated Ti-15Cu-25Ni (wt pct) foil produced joints with high nickel segregation and caused the formation of high amount of centerline alpha-two phase that contributed to the poor tensile behavior. In Reference 7, the brazing of dissimilar materials of Ti$_3$Al and Ti-6Al-4V (wt pct) alloys was carried out with Ti-Cu-Ni system fillers, and it was found that the presence of continuous Ti$_2$Ni phase deteriorated the joint strength. Furthermore, the joining of Ti$_2$AlNb and TiAl intermetallic alloys was conducted using diffusion bonding method,[8] and a new phase of Al(Nb, Ti)$_2$ was formed within the joint through a eutectoid-like reaction: Ti$_2$AlNb(B2) + Al → Al(Nb, Ti)$_2$+α_2 − Ti$_3$Al. The presence of Al(Nb, Ti)$_2$ with AlNb$_2$ structure deteriorated the mechanical properties of the joints. It should be noted that in this study, no interlayer was used. Although the maximum shear strength of 260 MPa for the joint bonded at 1273 K (1000 °C) was obtained at room temperature, a high bonding pressure of 20 MPa and a long dwell time of 60 min were needed in the experiment.[8] On the other hand, the joint properties at high temperatures were not reported.

It has been recognized that transient liquid-phase (TLP) diffusion bonding may combine the advantages of brazing and diffusion bonding, and sound joints can be available under lower joining temperatures.[9,10] Therefore, TLP diffusion bonding method has been used to join intermetallic alloys. For example, Zou et al.[11] investigated the TLP diffusion bonding of Ti-22Al-25Nb (at. pct) alloy using Ti-15Cu-15Ni (wt pct) foil and concluded that slow cooling after the bonding could modify the microstructure and improve the joints

H.S. REN, Ph.D. Candidate, is with the Department of Material Science and Engineering, Beihang University, Beijing 100191, China, and also with the Welding and Plastic Forming Division, Beijing Institute of Aeronautical Materials, Beijing 100095, China. H.P. XIONG, Professor, B. CHEN and X. WU, Senior Engineers, Y.Y. CHENG, Professor, and B.Q. CHEN, Doctor, are with the Welding and Plastic Forming Division, Beijing Institute of Aeronautical Materials. Contact e-mails: xionghp69@163.com and xionghuaping69@sina.cn S.J. PANG, Professor, is with the Department of Material Science and Engineering, Beihang University.

strength. However, these studies mainly focused on the joining of Ti$_3$Al-based alloy to itself or to Ti-based alloys.

In general, the service temperature of Ti$_3$Al-based alloy is about 923 K (650 °C), whereas TiAl intermetallics may offer a higher service temperature of 1033 K to 1123 K (760 °C to 850 °C). Besides, the plasticity of Ti$_3$Al-based alloy is much better than that of TiAl intermetallics.[12] Hence, in the case of high-temperature engineering application, the dissimilar joining of Ti$_3$Al to TiAl should be more attractive than Ti$_3$Al-Ti alloy combination.[13] Nevertheless, the study on the joining of Ti$_3$Al to TiAl is scarcely reported.

In this paper, an attempt was made to join Ti$_3$Al-based alloy to TiAl intermetallics by TLP diffusion bonding method. Considering the possible effect of heat cycles during the joining process on the mechanical properties of the base materials, bonding temperatures should be lower than the solid solution temperature [1243 K to 1263 K (970 °C to 990 °C)] of the Ti$_3$Al-based alloy. Therefore, in this study, a Ti-based alloy foil, Ti-13Zr-21Cu-9Ni (wt pct) which was usually used in the joining of Ti$_3$Al-based alloys and TiAl intermetallics themselves, was chosen as interlayer during the TLP diffusion bonding of the two base metals. Furthermore, this Ti-Zr-Cu-Ni interlayer alloy could be used under suitable bonding temperatures. Particularly, this study was intended to address the questions of whether using an interlayer foil can change the microstructure of the Ti$_3$Al/TiAl joints and thus improve the joint properties, and meanwhile whether the technical requirements for bonding experiments can be simplified compared with the dissimilar joints bonded without interlayer.

II. EXPERIMENTAL PROCEDURES

The Ti$_3$Al-based alloy to be joined was Ti-24Al-15Nb-1Mo (at. pct) alloy, composed of α_2-Ti$_3$Al, O-Ti$_2$AlNb and β/B2 phases. The nominal composition of the used TiAl intermetallics was Ti-48Al-2Cr-2Nb (at. pct) with a fully lamellar microstructure. The Ti-13Zr-21Cu-9Ni (wt pct) (Ti-21Zr-23Cu-9Ni at. pct) foil with a thickness of about 50 μm was fabricated by a rapid solidification technique, and double foil layers were laminated in the subsequent bonding experiment. Its liquidus temperature was 1161 K (888 °C) measured by differential thermal analysis (DTA).

Prior to bonding, surfaces to be joined were ground by SiC papers, and then the joined samples were ultrasonically cleaned in acetone. During the bonding experiment, the vacuum was kept between 7×10^{-3} and 8×10^{-4} Pa, and the heating rate was 0.2 K/s. Bonding temperature varied from 1173 K to 1233 K (900 °C and 960 °C), with a bonding time of 300 to 600 seconds and a fixed pressure of 2 MPa, followed by furnace cooling.

The mechanical characterization was performed by microhardness and shear strength. Microhardness test of various areas across the Ti$_3$Al/TiAl joints was performed using a Vickers hardness tester (450-SVD)

with a load of 50 g and load time of 15 seconds. At least three indentations were performed for each kind of microzone. The shear strength of the joint was measured at room temperature, 773 K and 873 K (500 °C and 600 °C), respectively. Details of the joint specimen and the illustration of the shear test are shown in Figure 1. The reported average strength was obtained from at least three specimens. The joint microstructures and the cross sections of the joints subjected to the shear test were examined using scanning electron microscope (SEM) equipped with an electron probe micro-analyzer (EPMA). Furthermore, the phase constitution of Ti$_3$Al/TiAl interface was identified using an X-ray diffraction (XRD) spectrometer detected not only on the as-fractured surface but also on its polished layer.

III. RESULTS AND DISCUSSION

A. Microstructure Evolution of Ti$_3$Al/TiAl Joints

Figure 2 shows the backscattered electron images of Ti$_3$Al/TiAl joints bonded with Ti-Zr-Cu-Ni interlayer using various bonding parameters. As can be seen, a lamellar structure consisted of white and black strips (as marked by "1" and "2" in Figure 2(b)) and a continuous reaction band ("3" in Figure 2(b)) are always visible adjacent to TiAl substrate within the joints. With the increase of bonding temperature, the lamellar structure and reaction band are thickened; for example, at the bonding temperature of 1193 K (920 °C), the lamellar structure and reaction band are only 7.9 and 2.2 μm, respectively (Figure 2(b)), but their thicknesses at 1233 K (960 °C) are increased to 13.4 and 5.8 μm, respectively (Figure 2(d)). Besides, evidently, there exists a white zone (like "5" in Figure 2(b)) in the center of the joints bonded at the lower bonding temperatures of 1173 K and 1193 K (900 °C and 920 °C). When the bonding temperature was increased to 1213 K or 1233 K (940 °C or 960 °C), such a white zone disappeared (Figures 2(c) and (d)). Additionally, when bonding at 1233 K (960 °C), some columnar α_2-Ti$_3$Al phase (microzone "8") precipitates within the center of the joint in Figure 2(d).

The EDS concentration profiles across the Ti$_3$Al/TiAl joint along the red line in Figure 2(b) are displayed in Figure 3. As shown in Figure 3(a), the content of element Al decreases gradually from the TiAl side to the joint center and presents an approximately uniform distribution in the center area. At the position $X = 15$ corresponding to "3" in Figure 2(b), concentration valleys are formed for the lines of elements Zr, Cu, and Ni, and peaks are visible for that of Ti and Al. Furthermore, at the position $X = 45$ corresponding to "5" in Figure 2(b), the content of Ti is the lowest and that of Zr, Cu, and Ni are the highest across the whole joint (Figure 3).

The EPMA map scanning results are also presented in Figure 4. Both Figures 3(a) and 4(a) demonstrate that the lamellar structure contains higher Al than other areas within the joint. EPMA analysis results in the
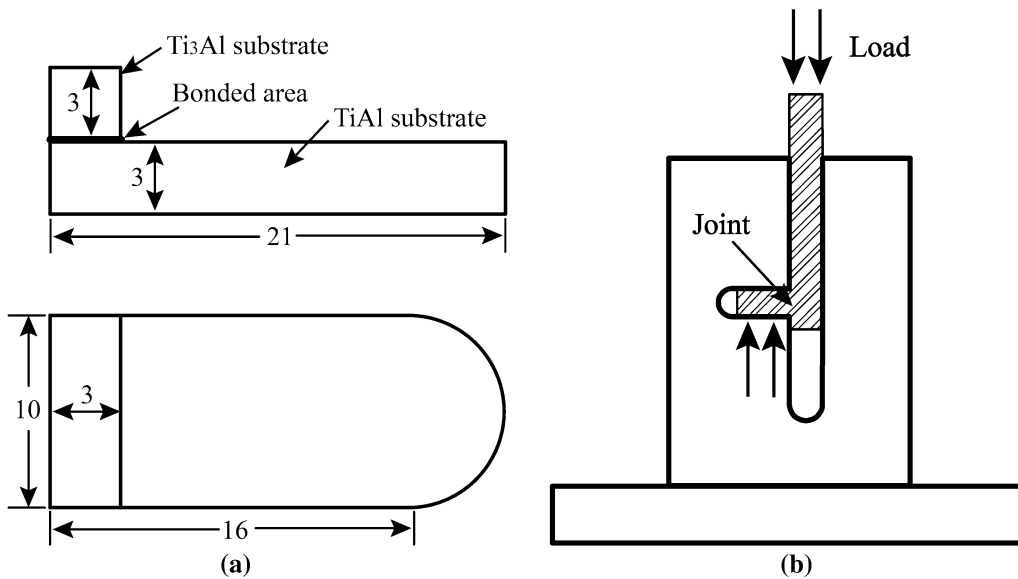
Fig. 1—Illustration of the shear test for the brazed joints: (a) geometry of shear test sample in mm; (b) shear test setup.
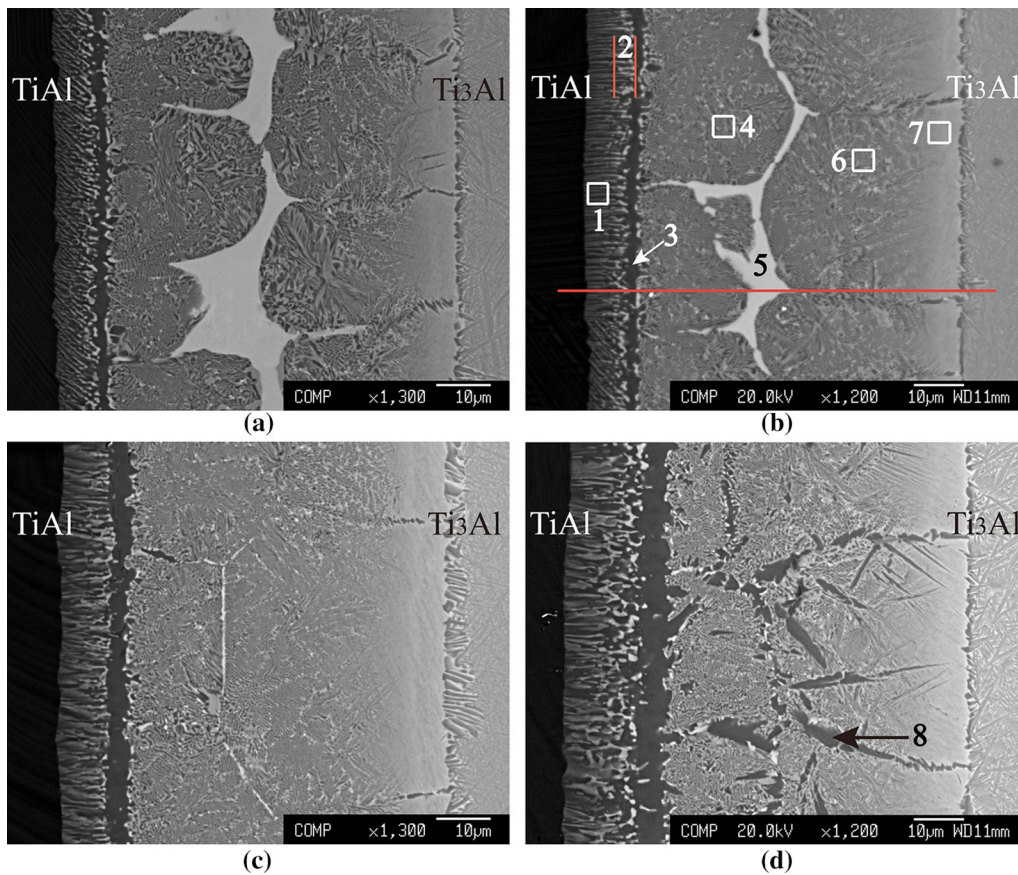

Fig. 2—Backscattered electron images of Ti₃Al/TiAl joints (bonding pressure: 2 MPa; dwell time: 600 s): (a) 1173 K (900 °C); (b) 1193 K (920 °C); (c) 1213 K (940 °C); (d) 1233 K (960 °C).

lamellar structure are listed in Table I, indicating the main elements of Ti and Al in microzones "1" and "2" (Figure 2(b)). As shown in Figure 2(b), the white strips in microzone "2" are thicker than that in microzone "1." The concentrations of Zr, Cu, and Ni in the former zone are a little higher (Table I). Thus, only slight difference exists between the white and black strips. In general, the phases in microzones "1" and "2"
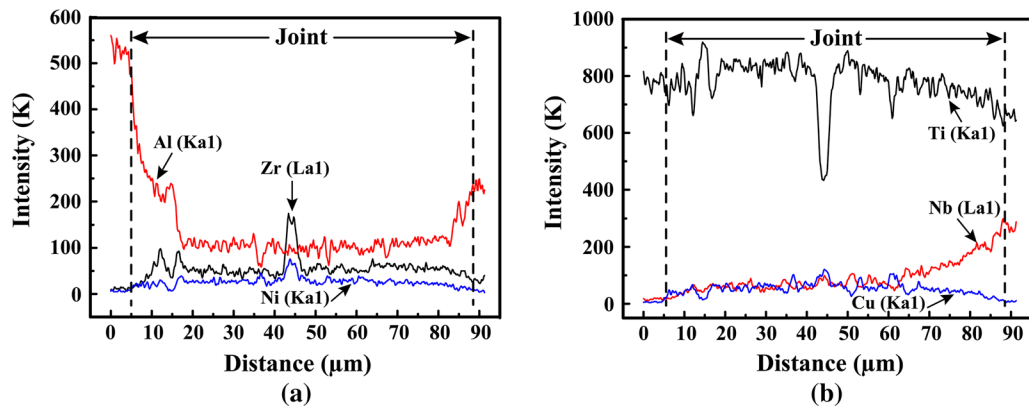
Fig. 3—Distribution profiles of major elements across the joint in Fig. 2(b).

(Figure 2(b)) are deduced to be Ti$_2$Al phase dissolved with Cu, Zr, and Ni. On the basis of References 14, 15, Ti$_2$Al was hexagonal with lattice parameters $a = 0.29$ nm and $c = 1.39$ nm and it was an intermediate phase during the phase transformation between α_2-Ti$_3$Al and γ-TiAl phases. Reference 16 also demonstrated the formation of Ti$_2$Al phase through the inter-diffusion reaction between Ti powder and TiAl powder during the hot-press sintering at 1473 K (1200 °C). In fact, in the present experiment, during the bonding process, Ti atoms diffused from the Ti-Zr-Cu-Ni interlayer alloy into the solid-state TiAl substrate due to the concentration gradient. Therefore, the Ti$_2$Al phase might be produced through the following diffusion reaction: Ti + TiAl = Ti$_2$Al. Undoubtedly, the diffusion velocity of atoms becomes faster as the bonding temperature increases. As a result, the Ti$_2$Al layer becomes thickened with the increase of bonding temperature, as shown in Figure 2.

Next, based on EPMA analysis results (Table I), the continuous reaction band ("3" in Figure 2(b)) can be identified as α_2-Ti$_3$Al phase, but it should be dissolved with low concentration of Zr, Cu, and Ni. According to the previous studies, the continuous α_2-Ti$_3$Al band was always formed when Ti-15Cu-15Ni (wt pct) filler alloy was used to join TiAl intermetallics to themselves or to Ti-based alloys.[17,18] In fact, the solubility of Zr, Cu, and Ni in α_2-Ti$_3$Al ordered structure is very limited, as confirmed by Table I and Figures 4(b) through (d). Then, once the continuous α_2-Ti$_3$Al band is formed, the further atomic inter-diffusion between TiAl substrate and the interface would be obstructed.[17] However, more Zr, Cu, and Ni are detected in microzone "2" than that in microzone "3" as shown in Figure 3 and Table I, signifying that the continuous α_2-Ti$_3$Al band should be resulted from solid-state phase transformation after the completion of solidification process.

At the bonding temperature, TiAl substrate will dissolve into the molten Ti-Zr-Cu-Ni interlayer alloy and α-phase containing high Al will be formed. Hence, it is deduced that due to the limited solubility of Al in the α-Ti at low temperature,[18,19] the α_2-Ti$_3$Al phase was probably formed through the ordering transformation of Al-rich α-Ti during cooling cycle. This is similar for the precipitation of the columnar α_2-Ti$_3$Al phase

(microzone "8" in Figure 2(d)) within the center of the joint in Figure 2(d). Undoubtedly, with the increase of bonding temperature, more TiAl substrate will dissolve into the molten Ti-Zr-Cu-Ni interlayer alloy. As a consequence, the thickness of the continuous α_2-Ti$_3$Al band in Figure 2 is increased gradually. During the formation of α_2-Ti$_3$Al band in microzone "3" (Figure 2(b)), Zr, Cu, and Ni are expelled to the neighbored areas. Finally, composition valleys at the position $X = 15$ are formed for the lines of elements Zr, Cu, and Ni, and peaks for that of Ti and Al (Figure 3).

As Table I indicated, the concentration of element Ti in the white zone (labeled by "5" in Figure 2(b)) is remarkably lower than other areas, and this is also demonstrated by Figures 3(a) and 4(e). Moreover, the contents of Zr, Cu, and Ni in this area are very close to that in the original interlayer filler. For these reasons, this white zone ("5" in Figure 2b) should be the residual Ti-Zr-Cu-Ni interlayer but it has been dissolved with Al. In order to further investigate the phase constitution of microzone "6" in Figure 2(b), the fractured surface of the joint subjected to shear test (see Section III–B below) was polished off 10 to 20 μm and then analyzed again by XRD. The corresponding XRD pattern in Figure 5 together with Table I signifies that microzone "6" in Figure 2(b) is mainly composed of Ti-rich phase, α_2-Ti$_3$Al and Ti$_2$Cu, which is similar to microzone "4" (Figure 2(b)). Besides, microzone "7" in Figure 2(b) could be considered as a mixture of Ti-rich phase dissolved with Cu and O-Ti$_2$AlNb.

In addition, a short bonding time of 300 s with Ti-Zr-Cu-Ni interlayer was also tested for the Ti$_3$Al/ TiAl joint. The corresponding interfacial microstructure and EPMA analysis results in microzones are shown in Figure 6 and Table II, respectively. Compared with the joint bonded at 1193 K(920 °C)/2 MPa/600 seconds (Figure 2(b)), more residual interlayer dissolved with Al (microzone "4" in Figure 6) was retained due to the less diffusion time. However, the thicknesses of lamellar structure and α_2-Ti$_3$Al band are close to that in Figure 2(b).

During the bonding process, the dissolution of TiAl or Ti$_3$Al substrate into the molten interlayer and the diffusion of alloying elements Zr, Cu, and Ni from the interlayer into the TiAl or Ti$_3$Al substrate would
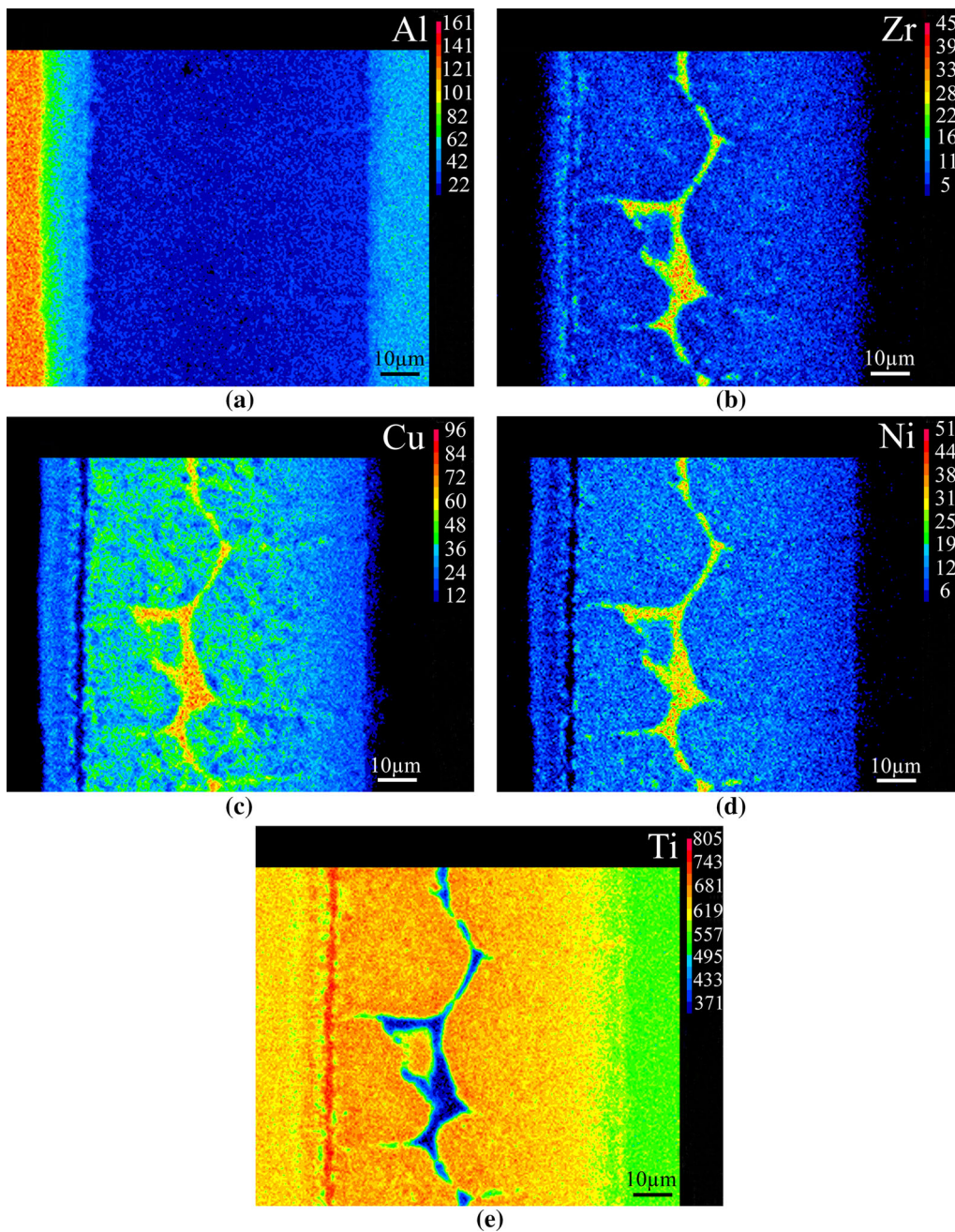
Fig. 4—EPMA map scanning results of Al (*a*), Zr (*b*), Cu (*c*), Ni (*d*), and Ti (*e*) in Fig. 2(b).

Table I. EPMA Analysis Results for the Microzones in Fig. 2, at. pct

Microzones	Ti	Al	Zr	Cu	Ni	Cr	Nb	Deduced Phases
1	62.90	26.90	1.72	5.82	1.81	0.84	—	Ti$_2$Al dissolved with Cu
2	61.64	25.04	3.81	6.95	2.18	0.38	—	Ti$_2$Al dissolved with Cu
3	70.82	23.78	1.99	1.90	0.54	—	0.97	α_2-Ti$_3$Al
4	70.46	11.87	2.37	9.49	3.35	0.36	2.10	Ti-rich phase + α_2-Ti$_3$Al + Ti$_2$Cu
5	39.42	13.09	13.84	22.75	10.59	0.31	—	residual interlayer dissolved with Al
6	69.18	11.53	3.01	9.42	3.71	0.38	2.77	Ti-rich phase + α_2-Ti$_3$Al + Ti$_2$Cu
7	67.94	13.35	2.04	6.54	2.58	—	7.55	Ti-rich phase dissolved with Cu + O-Ti$_2$AlNb
8	70.82	19.64	1.73	1.57	0.53	—	5.72	α_2-Ti$_3$Al dissolved with Nb

gradually change the composition of the molten inter-layer alloy and therefore continuously increase its liquidus temperature. Once the liquidus temperature reached the bonding temperature, isothermal solidification started.[20] Microzones "4", "6," and "7" (Figure 2(b)) were thus formed. If the joint was cooled down before the completion of the isothermal solidification, some molten interlayer alloy would be reserved. It would be solidified once the temperature reached its melting point. Due to the high concentration of melting point depressants (Zr, Cu, and Ni), residual interlayer dissolved with Al (microzone "5" in Figure 2(b)) should be athermal solidification zone.
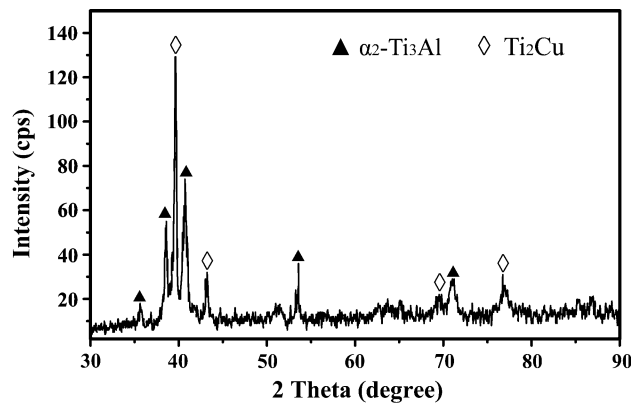

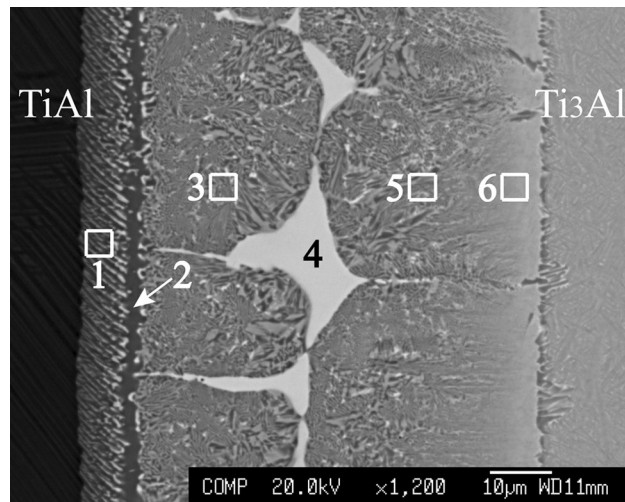Fig. 5—XRD pattern of the zone labeled by "6" in Fig. 2(b).

Fig. 6—Backscattered electron images of Ti₃Al/TiAl joints bonded at 1193 K(920 °C)/2 MPa/300 s.

In general, the Ti₃Al/TiAl joint TLP diffusion bonded at 1193 K (920 °C) mainly consisted of Ti-rich phase, Ti₂Al layer, α₂-Ti₃Al band, and residual interlayer alloy dissolved with Al. This is very different from the Ti₂AlNb/TiAl joint obtained by diffusion bonding method without interlayer.[8] As presented in Reference 8, when bonded at low temperature [1223 K (950 °C)], Al(Nb, Ti)₂ and α₂-Ti₃Al particles were formed alternately at the interface adjacent to the Ti₂AlNb base alloy. In contrast, at relatively high temperature [1273 K (1000 °C)], a B2-enriched zone was found adjacent to the Ti₂AlNb base alloy. The presence of either Al(Nb, Ti)₂ or the B2-enriched zone, to some extent, would impair the mechanical properties of the Ti₂AlNb/TiAl joints. Particularly, a continuous α₂-Ti₃Al layer was always visible at the interface adjacent to the joined TiAl intermetallics, which was similar to the TLP diffusion-bonded Ti₃Al/TiAl joints in this study. It should be noted that the total thickness of the Ti₂AlNb/TiAl joint bonded in Reference 8 was about 20 μm, in which the continuous α₂-Ti₃Al reaction layer reached a 10-μm thickness, thus increasing the joint brittleness intensively. On the contrary, in this study as shown in Figure 2(b), the thickness of α₂-Ti₃Al band is only about 2.2 μm and Ti-rich phase dominates the most areas of the joint.

B. Mechanical Properties of Ti₃Al/TiAl Joints

Figure 7 shows the room-temperature shear strength of the joints with the bonding time of 600 seconds as a function of bonding temperatures. The bonding temperature of 1173 K (900 °C) offers a shear strength of 339 MPa. In particular, when the bonding temperature is increased to 1193 K (920 °C), the joint strength even reaches the maximum value of 417 MPa. However, further increase of bonding temperature results in the decrease of the joint strength, that is, as the bonding temperature is raised to 1233 K (960 °C), the joint strength has been decreased to 145 MPa. In the case of the change of bonding time, the joint bonded at 1193 K(920 °C)/2 MPa/300 seconds presents a shear strength of 364 MPa at room temperature, lower than that for 600 s.

As previously described, the Ti₂AlNb/TiAl joint diffusion bonded without interlayer exhibited a shear strength of 260 MPa at room temperature.[8] It is clear that the TLP diffusion bonding method using Ti-Zr-Cu-Ni foil as interlayer has remarkably elevated the strength of the dissimilar joint. On the other hand, for this bonding method, only a low pressure of 2 MPa and

Table II. EPMA Analysis Results for the Microzones in Fig. 6, at. pct

| Microzones	Ti	Al	Zr	Cu	Ni	Cr	Nb	Deduced Phases
1	60.46	27.27	1.73	6.27	3.22	1.05	—	Ti₂Al dissolved with Cu
2	73.42	22.67	1.14	2.10	0.67	—	—	α₂-Ti₃Al
3	69.28	11.47	2.71	10.30	3.51	0.46	2.27	Ti-rich phase + α₂-Ti₃Al + Ti₂Cu
4	53.93	10.82	8.52	17.55	8.71	0.47	—	residual interlayer dissolved with Al
5	67.90	11.85	2.67	9.98	3.19	0.45	3.96	Ti-rich phase + α₂-Ti₃Al + Ti₂Cu
6	67.91	12.23	1.41	6.84	2.68	—	8.93	Ti-rich phase dissolved with Cu + O-Ti₂AlNb
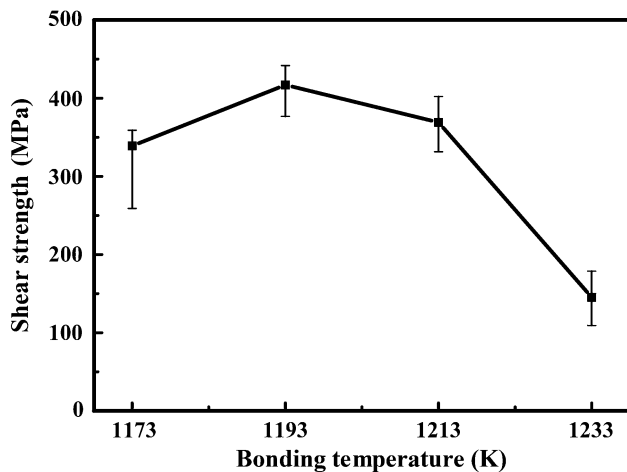
Fig. 7—Effect of bonding temperature on room-temperature shear strength of the Ti₃Al/TiAl joints (bonding pressure: 2 MPa; dwell time: 600 s).

a short diffusion time of 300 to 600 seconds are needed. Therefore, using the Ti-Zr-Cu-Ni interlayer has simplified the technical requirements to a great extent compared with the dissimilar joints bonded without interlayer.[8] In addition, according to the measured results at high temperatures for the joints bonded at 1193 K (920 °C) for 600 seconds, the shear strengths of 234 and 164 MPa were maintained at 773 K and 873 K (500 °C and 600 °C), respectively.

In order to identify the fracture mechanism of the Ti₃Al/TiAl joints, the specimens after shear tests are inspected. As shown in Figure 8(a), the crack mainly propagates along the white phase (residual interlayer dissolved with Al, Figure 2(b)). As mentioned above, the white phase is the athermal solidification zone. The continuous distributed athermal solidification zone can cause stress concentration and provide a low resistance path for crack initiation or propagation as reported in some alloys.[21,22] On the other hand, the XRD pattern (Figure 9) of the as-fractured surface confirms the presence of Ti₂Al and α₂-Ti₃Al phases as well as intermetallic compounds of Ti₂Ni and Ti(Cu, Al)₂. Based on Table I, the two compounds of Ti₂Ni and Ti(Cu, Al)₂ should be formed within the residual interlayer dissolved with Al ("5" in Figure 2(b)). Considering the fracture characteristic, this residual interlayer zone is just the weak link within the joint, which is attributed to the intensive formation of Ti₂Ni and Ti(Cu, Al)₂ compounds.

For the joint bonded at 1233 K (960 °C), it fractures along the Ti₂Al layer and/or the continuous α₂-Ti₃Al band (Figure 8(b)). As can be seen in Figure 2(d), the residual interlayer has disappeared; but the Ti₂Al layer and α₂-Ti₃Al band are thickened. The Ti₂Al layer contains high Al and presents a lamellar structure similar to the TiAl substrate. It might exhibit a strong brittleness tendency and should be detrimental to joint strength. Furthermore, α₂-Ti₃Al phase is of inherent brittleness,[17] its continuous distribution would lead to
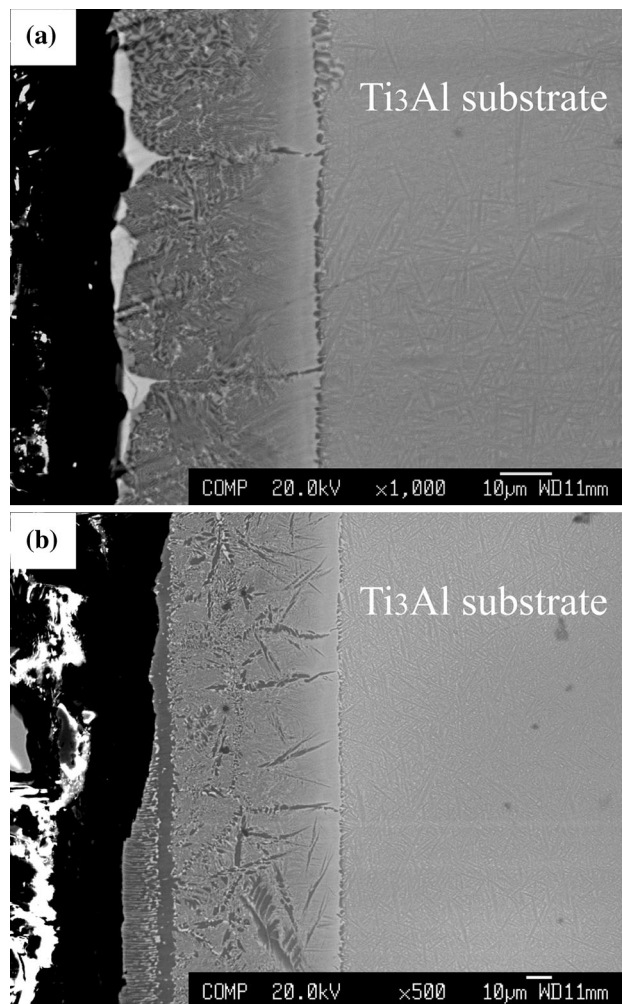

Fig. 8—Cross sections of Ti₃Al/TiAl joints after shear tests, Ti₃Al side (bonding pressure: 2 MPa; dwell time: 600 s): (a) 1193 K (920 °C); (b) 1233 K (960 °C).

stress concentration during the shear test and thus deteriorate the joint strength.

The microhardness profile along the cross section of the joint bonded at 1193 K (920 °C) for 600 seconds is displayed in Figure 10. In general, the whole joint exhibits higher microhardness than the two base materials. The hardness value in Ti₂Al layer (microzones "1" and "2" in Figure 2(b)) is slightly higher than that of microzones "4" and "6" in Figuure 2(b). The maximum hardness (661 HV) appears within the residual interlayer dissolved with Al (labeled "5" in Figure 2(b)). According to previous studies, the hardness of Ti(Cu, Al)₂ was 597 HV.[23] and that of Ti₂Ni was even high up to 700 HV.[24] Therefore, it is not strange that the residual interlayer dissolved with Al corresponds to the maximum hardness value.

Evidently, due to the high hardness, the excessive residual interlayer in Figure 2a would be detrimental to the joint strength. With the increase of bonding temperature, strong dissolution and inter-diffusion between base metals and molten Ti-Zr-Cu-Ni alloy occur. The amount of the hard residual interlayer is reduced, and
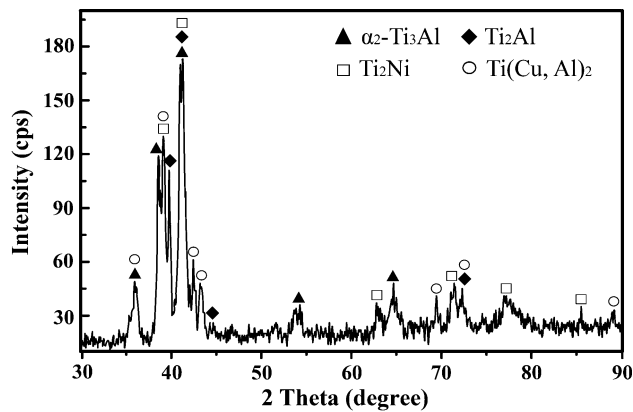
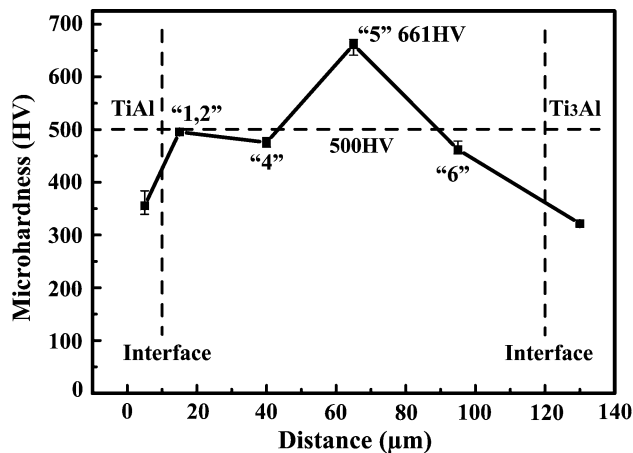Fig. 9—XRD pattern of the fractured surface after shear test for specimen bonded at 1193 K(920 °C)/2 MPa/600 s.

Fig. 10—Microhardness profile along the cross section of the Ti₃Al/ TiAl joint (Fig. 2(b)) bonded at 1193 K(920 °C)/2 MPa/600 s.

this would decrease stress concentration tendency and joint brittleness. Hence, the joint bonded at 1193 K (920 °C) shows a higher shear strength than that bonded at 1173 K (900 °C). But for the joints bonded at 1213 K and 1233 K (940 °C and 960 °C) as shown in Figures 2(c) and (d), although the residual interlayer disappears, the thickened Ti_2Al layer and α_2-Ti_3Al band conversely deteriorate the joint strength (Figure 8(b)).

Although the shear strengths of 417 MPa at room temperature and 234 MPa at 500 °C have been acquired using the Ti-Zr-Cu-Ni interlayer alloy, the joint properties including high-temperature strength should be improved. And further studies searching for new interlayer alloys are still needed for achieving a stronger joining of Ti_3Al-based alloy to other materials.[25–28]

IV. CONCLUSIONS

Microstructure evolution and bonding strength of TLP diffusion-bonded Ti_3Al/TiAl joints using Ti-13Zr-21Cu-9Ni (wt pct) foil as interlayer have been investigated in this study. Primary conclusions are summarized as the follows:

1. The joint mainly consisted of Ti-rich phase, Ti_2Al layer, α_2-Ti_3Al band, and residual interlayer dissolved with Al. The amount of residual interlayer at the central part of the joint was decreased with the increase of the bonding temperature. In the meantime, the Ti_2Al and α_2-Ti_3Al reaction bands were thickened gradually and some columnar α_2-Ti_3Al phases precipitated within Ti-rich areas.

2. The whole joint exhibited a higher microhardness than the two base materials, and the residual interlayer at the central part of the joint showed the maximum microhardness across the whole joint. The joint bonded under the condition of 1193 K (920 °C)/2 MPa/600 seconds presented the maximum shear strength of 417 MPa at room temperature, and the strength of 234 MPa was maintained at 773 K (500 °C).

3. Ti-rich phase dominated the most areas of the TLP diffusion-bonded Ti_3Al/TiAl joints, the joint properties were improved to a great extent, and the technical requirements for bonding experiments were simplified compared with the dissimilar joints bonded without interlayer.

REFERENCES

1. A. Lasalmonie: *Intermetallics*, 2006, vol. 14, pp. 1123–29.
2. A.S. Ramos, M.T. Vieira, M.F. Vieira, and F. Viana: *Mater. Sci. Forum*, 2006, vols. 514–6, pp. 483–89.
3. Y. Wu, D.Z. Yang, and G.M. Song: *Intermetallics*, 2000, vol. 8, pp. 629–32.
4. A.P. Wu, G.S. Zou, J.L. Ren, H.J. Zhang, G.Q. Wang, X. Liu, and M.R. Xie: *Intermetallics*, 2002, vol. 10, pp. 647–52.
5. L.J. Tan, Z.K. Yao, W. Zhou, H.Z. Guo, and Y. Zhao: *Aerosp. Sci. Technol.*, 2010, vol. 14, pp. 302–6.
6. C.H. Cadden, N.Y.C. Yang, and T.H. Headley: *Weld. J.*, 1997, vol. 76, pp. 316–25.
7. R.K. Shiue, S.K. Wu, and Y.T. Chen: *Intermetallics*, 2010, vol. 76, pp. 107–14.
8. J.Y. Zou, Y.Y. Cui, and R. Yang: *J. Mater. Sci. Technol.*, 2009, vol. 25, pp. 819–24.
9. W.D. Macdonald and T.W. Eagar: *Annu. Rev. Mater. Sci.*, 1992, vol. 22, pp. 23–46.
10. M. Mosallaee, A. Ekrami, K. Ohsasa, and K. Matsuura: *Metall. Mater. Trans. A*, 2008, vol. 39A, pp. 2389–2402.
11. G.S. Zou, E.H. Xie, H.L. Bai, A.P. Wu, Q. Wang, and J.L. Ren: *Mater. Sci. Eng. A*, 2009, vol. 499, pp. 101–05.
12. S.L. Shu, F. Qiu, C.Z. Tong, X.N. Shan, and Q.C. Jiang: *J. Alloys Compd.*, 2014, vol. 617, pp. 302–05.
13. H.P. Xiong, J.Y. Mao, B.Q. Chen, Q. Wang, S.B. Wu, and X.H. Li: *J. Mater. Eng.*, 2013, vol. 10, pp. 1–12 (in Chinese).
14. S.J. Yang and S.W. Nam: *Mater. Sci. Eng. A*, 2002, vols. 329–331, pp. 898–905.
15. G.H. Cao, W. Skrotzki, and T. Gemming: *J. Alloys Compd.*, 2006, vol. 417, pp. 169–72.
16. H.P. Xiong, Q. Shen, J.G. Li, and L.M. Zhang: *J. Mater. Sci. Lett.*, 2000, vol. 19, pp. 989–93.

17. S.J. Lee and S.K. Wu: *Intermetallics*, 1999, vol. 7, pp. 11–21.
18. R.K. Shiue, S.K. Wu, Y.T. Chen, and C.Y. Shiue: *Intermetallics*, 2008, vol. 16, pp. 1083–89.
19. S.J. Lee, S.K. Wu, and R.Y. Lin: *Acta Mater.*, 1998, vol. 46, pp. 1297–1305.
20. M. Pouranvari, A. Ekrami, and A.H. Kokabi: *J. Alloys Compd.*, 2008, vol. 461, pp. 641–47.
21. A.A. Ghoneim and O.A. Ojo: *Metall. Mater. Trans. A*, 2012, vol. 43A, pp. 900–11.
22. O.A. Idowu, O.A. Ojo, and M.C. Chaturvedi: *Metall. Mater. Trans. A*, 2006, vol. 37A, pp. 2787–96.
23. R.K. Shiue, S.K. Wu, and S.Y. Chen: *Acta Mater.*, 2003, vol. 51, pp. 1991–2004.
24. H. Hiraga, T. Inoue, H. Shimura, and A. Matsunawa: *Wear*, 1999, vol. 231, pp. 272–78.
25. H.S. Ren, H.P. Xiong, B. Chen, and S.J. Pang: *Weld. World*, 2015, vol. 59, pp. 639–46.
26. H.S. Ren, H.P. Xiong, B. Chen, S.J. Pang, B.Q. Chen, and L. Ye: *J. Mater. Process. Tech.*, 2015, vol. 224, pp. 26–32.
27. B.Q. Chen, H.P. Xiong, B.B. Sun, B.R. Du, Z.W. Wei, and B. Chen: *Mater. Des.*, 2015, vol. 87, pp. 732–41.
28. H.S. Ren, H.P. Xiong, B. Chen, S.J. Pang, X. Wu, Y.Y. Cheng, and B.Q. Chen: *Mater. Sci. Eng. A*, 2016, vol. 651, pp. 45–54.